Available online at www.sciencedirect.com
ScienceDirect
Journal of Molecular Catalysis A: Chemical 266 (2007) 149–157
JOURNAL OF MOLECULAR CATALYSIS A: CHEMICAL
www.elsevier.com/locate/molcata

Photocatalytic activity of La-doped ZnO for the degradation of monocrotophos in aqueous suspension

S. Anandan [a], A. Vinu [a,*], K.L.P. Sheeja Lovely [b], N. Gokulakrishnan [c], P. Srinivasu [a], T. Mori [a], V. Murugesan [d], V. Sivamurugan [d], K. Ariga [c]

[a] *Nano-ionics Materials Group, Fuel Cell Materials Center, National Institute for Materials Science, 1-1 Namiki, Tsukuba, Ibaraki 305-0044, Japan*
[b] *Department of Chemistry, Annamalai University, Annamalai Nagar 608 002, India*
[c] *Supermolecules Group, Advanced Materials Laboratory, National Institute for Materials Science, 1-1 Namiki, Tsukuba, Ibaraki 305-0044, Japan*
[d] *Department of Chemistry, Anna University, Chennai 600 025, India*

Received 17 October 2006; received in revised form 1 November 2006; accepted 1 November 2006
Available online 10 November 2006

Abstract

La-doped ZnO nanoparticles with different La contents were synthesized and characterized by various sophisticated techniques such as XRD, UV–vis, AFM, XPS, and HR-SEM. The XRD results revealed that La^{3+} is uniformly dispersed on ZnO nanoparticles in the form of small La_2O_3 cluster. It was found that the particle size of La-doped ZnO is much smaller as compared to that of pure ZnO and decreases with increasing La loading. Rough and high porous surface of La-doped ZnO was observed by AFM, which is critical for enhancing the photocatalytic activity. The photocatalytic activity of La-doped ZnO in the degradation of monocrotophos (MCP) was studied. The effects of the adsorption of MCP, lights of wavelength, and the solution pH on the photocatalytic activity of La-doped ZnO with different La loading were studied and the results were compared with pure ZnO and pure TiO_2. It was observed that the rate of degradation of MCP over La-doped ZnO increases with increasing La loading up to 0.8 wt% and then decreases. It was found that the doping of La in ZnO helps to achieve complete mineralization of MCP within a short irradiation time. Among the catalyst studied, the 0.8 wt% La-doped ZnO was the most active, showing high relative photonic efficiencies and high photocatalytic activity for the degradation of MCP.

Keywords: Monocrotophos; La-doped ZnO; Photocatalytic degradation; Relative photonic efficiency

1. Introduction

Metal oxide semiconductor materials, such as TiO_2, ZnO have attracted considerable attention in the recent year owing to their photocatalytic ability in the degradation of various environmental pollutants, such as pesticides, detergents, dyes, and volatile organic compounds into carbon dioxide, water, and mineral acids under UV light irradiation [1–4]. Although TiO_2 is universally recognized as the most photo active catalyst, ZnO is a suitable alternative to TiO_2 as it has similar band gap energy (3.2 eV) [5] and its lower cost and better performance in the degradation of organic dye molecule in both acidic and basic medium than TiO_2 has stimulated many researchers to further explore the properties of this oxide in many photocatalytic reactions [6–9]. It has been recently shown that ZnO colloids are more effective in production of H_2O_2 and photocatalytic degradation of organic acids than TiO_2 colloids. In addition, the emitting properties of ZnO, which are developed in the system due to various kinds of intrinsic defects such as oxygen vacancies, zinc vacancies, zinc interstitials, oxygen interstitials, and antisite defect, can help to set up a catalytic system which is able to sense and shoot environmental contaminants [10–12].

ZnO has also several drawbacks including the fast recombination rate of photogenerated electron–hole pair and a low quantum yield in the photocatalytic reactions in aqueous solutions, which obstruct commercialization of the photocatalytic degradation process [13,14]. Consequently, there has been a lot of interest in improving the photocatalytic activity by suitable modification of semiconductors for the degradation of organic compounds in water. It has been found that the interfacial electron transfer efficiency and rate of the recombination of electron–hole pairs of semiconductor materials can be easily tuned by various surface

* Corresponding author. Tel.: +81 29 860 4563; fax: +81 29 860 4667.
E-mail address: vinu.ajayan@nims.go.jp (A. Vinu).

1381-1169/$ – see front matter © 2006 Elsevier B.V. All rights reserved.
doi:10.1016/j.molcata.2006.11.008

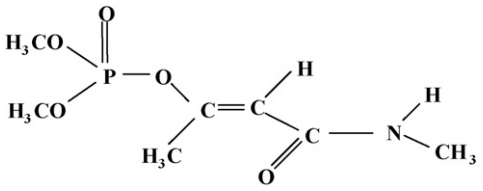

Fig. 1. Structure of monocrotophos (MCP).

modification methods such as surface chelation, surface derivatization, platinization, and selective metal ion and nitrogen doping [15–20]. It has been also demonstrated that the presence of heavy metals such as Pt, Pd, Au, and Ag on semiconducting metal oxides or zeolite supported TiO_2 can enhance the degradation efficiency of photocatalytic reactions [21–28]. Very recently, La-doped TiO_2 nanoparticle has attracted much attention in the photocatalytic processes owing to its high photocatalytic activity in the degradation of organic contaminants because of the suppression of electron–hole recombination, large content of oxygen vacancies, and strong absorption of OH^- ions on the surface of the catalyst [23–25]. Unfortunately, there has been no report available on the preparation of rare earth-doped ZnO nanoparticles and their photocatalytic activities towards the degradation of pollutants present in water though it has almost similar band gap energy as that of TiO_2.

MCP is a model pollutant (Fig. 1), which is identified as endocrine disrupting chemicals (EDCs). Endocrine disrupting chemicals (EDCs), an exogenous agent present in the environment, disrupt the endocrine functions such as growth, development and reproduction of humans and animals. Recent research reports [29] have highlighted the existence of these chemicals in surface and ground water via point and non-point sources. A few adverse effects of EDCs are early maturity, defect in child birth and impotence [30]. Hence, the treatment of wastewater containing endocrine disrupting chemicals is imperative.

Here we report for the first time on the synthesis and characterization of La-doped ZnO catalysts and their photocatalytic activity on the degradation of. MCP. All the materials have been unambiguously characterized by XRD, FT-IR, UV–vis, XPS, AFM, and HR-SEM analysis. It has been found that the photocatalytic activity of La-doped ZnO is much higher as compared to that of pure ZnO and TiO_2. Moreover, La-doped ZnO photocatalysts require shorter irradiation time for complete mineralization than pure ZnO and TiO_2. The relative photonic efficiency of ZnO, TiO_2, and La-doped ZnO has also been compared and the results have been discussed. Interestingly, the relative photonic efficiency of La-doped ZnO is much higher as compared to that of pure ZnO and TiO_2.

2. Experimental

2.1. Materials

Zinc nitrate hexahydrate ($Zn(NO_3)_2{\cdot}6H_2O$) (Analytical grade, Merck Ltd., India) and lanthanum nitrate hexahydrate ($La(NO_3)_3{\cdot}6H_2O$) (Analytical grade, CDH, India) were used as zinc and lanthanum sources, respectively. Sodium carbonate anhydrous (Na_2CO_3) was purchased from Merck (Analytical grade), India. The technical grade sample of monocrotophos (MCP) was received from Sree Ramcides Chemicals, India. HPLC grade acetonitrile was purchased from Merck, India. All the chemicals were used without further purification.

2.2. Preparation of photocatalysts

La-doped ZnO nanoparticles were prepared by co-precipitation method using the precursors of zinc and lanthanum. $Zn(NO_3)_2{\cdot}6H_2O$ and Na_2CO_3 were dissolved separately in double distilled water to obtain 0.5 mol/l solutions. Zinc nitrate solution (250 ml of 0.5 mol/l) was slowly added into vigorously stirred 250 ml of 0.5 mol/l Na_2CO_3 solution. Lanthanum nitrate in the required stoichiometry was slowly added into the above solution and a white precipitate was obtained. The precipitate was filtered, repeatedly rinsed with distilled water, and then washed twice with ethanol. The resultant solid product was dried at 100 °C for 12 h and calcined at 300 °C for 2 h. ZnO particles were also prepared by the same procedure without the addition of lanthanum nitrate solution. The doping concentrations of lanthanum are expressed in wt%.

2.3. Characterization of photocatalysts

The crystallinity of pure ZnO and La-doped ZnO catalysts were analyzed by X-ray powder diffraction using PANalytical X-ray diffractometer with Cu Kα radiation in the scan range 2θ between 10° and 70°. An accelerating voltage of 40 kV and an emission current of 25 mA were used. The UV–vis spectra of pure ZnO and La-doped ZnO catalysts were recorded in the range 200–700 nm using Shimadzu, Model: UV-1601. For recording of the spectra, the catalyst (~5 mg) in paraffin oil (2 ml) was finely crushed and applied over Whatman 40 filter paper. The absorbance spectra were then recorded in the range 200–700 nm for all the catalysts using a filter paper soaked in paraffin oil as the reference.

Pure ZnO and La-doped ZnO surfaces were investigated by an atomic force microscope (Model: Digital Instruments, 3100). The samples were analyzed by contact mode with Si_3N_4 tip having a force constant of 0.12 N/m. The presence of elements and chemical states of the catalysts were examined by ESCALAB 200 X-ray photoelectron spectrophotometer (VG Scientific) with monochromatic Mg Kα excitation source. The pressure was maintained at 6.3×10^{-5} Pa. Prior to XPS measurements all as-sprayed samples were calcined at 673 K for 2 h to ensure that any possible residual precursors would decompose completely. The texture and morphology of pure ZnO and La-doped ZnO were measured by a high resolution-scanning electron microscope (Hitachi, Model: S-4800).

2.4. Adsorption studies

Prior to photocatalytic experiments, the adsorption of MCP on ZnO and La-doped ZnO catalysts was carried out by mixing 100 ml of aqueous solution of MCP with fixed weight of

the respective catalyst (100 mg). This slurry was equilibrated for 30 min in a magnetic stirrer. The aqueous MCP solution was then separated from the catalyst by centrifugation and the change in MCP concentration was measured by HPLC. The amount of adsorption of MCP on ZnO and La-doped ZnO catalysts was calculated by comparing the concentration before and after stirring. From the adsorption experiments, the percentage of MCP adsorbed on the catalyst surface was determined from the following equation:

$$\%\ \text{of adsorption} = \frac{C_0 - C_t}{C_0}$$

where C_0 is the initial concentration of MCP and C_t is the concentration of MCP after 't' minutes.

2.5. Photocatalytic reactor setup and degradation procedure

The cylindrical photochemical reactor tube was made up of quartz with a dimension of 30 cm × 3 cm (height × diameter). The top portion of the reactor tube has ports for sampling, gas purging, and gas outlet. The aqueous pesticide solution containing appropriate quantity of either pure ZnO or La-doped ZnO was taken in the quartz reactor and subjected to aeration for thorough mixing. The reactor tube was placed inside the reactor setup and the distance between the reactor set up and the UV lamp was adjusted to 6.5 cm. The lamp housing consisted of low-pressure mercury lamps (8 × 8 W) emitting either 254 or 365 nm with polished anodized aluminum reflectors and black cover to prevent UV leakage. The photocatalytic degradation was carried out by mixing 100 ml of aqueous MCP solution and 100 mg of pure ZnO or La-doped ZnO photocatalyst. The experiments were performed at room temperature and the pH of the reaction mixture was kept at 5.4. Prior to irradiation, the slurry was aerated for 30 min to reach adsorption equilibrium followed by UV irradiation. Aliquots were withdrawn from the suspension at specific time intervals and centrifuged immediately at 1500 rpm. Then it was filtered through a 0.2 μm millipore filter paper to remove suspended particles. The filtrate was analyzed by HPLC and TOC to find out the extent of degradation and mineralization of MCP.

2.6. Analytical methods

The concentration of MCP was analyzed by HPLC instrument (Shimadzu, Model: SPD-10A VP) with a UV-Vis detector. In the HPLC analysis, Shim-pack CLC-C8 column (5 μm particle size, 250 mm length and 4.6 mm inner diameter) and mobile phase of acetonitrile/water (6:4, v/v) was used with a flow rate of 1.0 ml min^{-1}. An injection volume of 20 μl was used. The total organic carbon was determined by a TOC analyzer (Shimadzu, Model: 5000A) equipped with a single injection auto sampler (ASI-5000).

2.7. Relative photonic efficiency (ξ_r)

The relative photonic efficiency of the catalyst is obtained by comparing the photonic efficiency of La-doped ZnO with that of the standard photocatalyst (ZnO—Merck). In order to evaluate ξ_r, a solution of MCP (40 mg l^{-1}) with a pH of 10 was irradiated with 100 mg of ZnO or La-doped ZnO for 60 min. From the degradation results, ξ_r was calculated as follows:

$$\xi_r = \frac{\text{initial rate of MCP degradation on La-doped ZnO}}{\text{initial rate of MCP degradation on pure ZnO}}$$

where both initial rates were obtained exactly under identical conditions.

3. Results and discussion

3.1. Characterization of photocatalysts

3.1.1. XRD patterns of ZnO and La-doped ZnO

The powder X-ray diffraction patterns of ZnO and La-doped ZnO with different lanthanum contents are shown in Fig. 2. The particle size, unit cell parameter and unit cell volume are presented in Table 1. The XRD patterns of all the La-doped ZnO catalysts are almost similar to that of ZnO [31], suggesting that there is no change in the crystal structure upon La loading. This also indicates that La^{3+} is uniformly dispersed on ZnO nanoparticles in the form of small La_2O_3 cluster. However, it should be noted that the La-doped samples have a wider and lower intense diffraction peaks than pure ZnO. Moreover, the XRD peaks of La-doped ZnO continuously get broader with increasing the La loading. It is interesting to note that the particle size of La-doped ZnO calculated using Scherrer equation is much smaller as compared with that of the pure ZnO, which decreases with increasing the La loading. The decrease in the particle size of La-doped ZnO is mainly attributed to the formation of La–O–Zn on the surface of the doped samples, which hinders the growth of crystal grains [17].

3.1.2. UV–visible (UV–vis) analysis

The UV–vis absorption spectra of ZnO and La-doped ZnO are shown in Fig. 3. The absorbance maxima and the corresponding band gap values and the rate constants for the degradation of MCP for all the catalysts are presented in Table 2. It can be clearly seen from Fig. 3 that the maximum of the absorbance

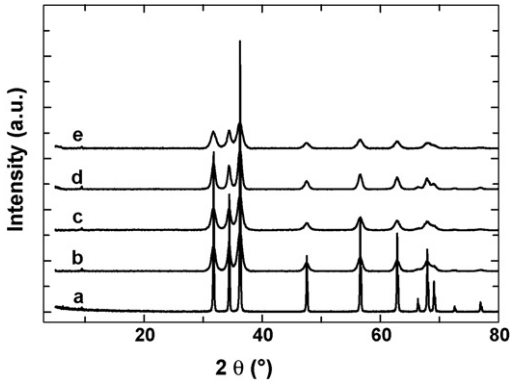

Fig. 2. XRD patterns of ZnO and La-doped ZnO: (a) pure ZnO, (b) 0.2 wt% La-doped ZnO, (c) 0.5 wt% La-doped ZnO, (d) 0.8 wt% La-doped ZnO, and (e) 1.0 wt% La-doped ZnO.

Table 1
Physical characteristics of pure ZnO and La-doped ZnO catalysts

Catalysts	Crystal size (nm)	Lattice parameter (*a*) (nm)	Lattice parameter (*c*) (nm)	Unit cell volume (nm^3)
Pure ZnO	53.11	0.3248	0.5205	0.0476
0.2% La–ZnO	45.44	0.3255	0.5143	0.0478
0.5% La–ZnO	23.60	0.3259	0.5171	0.0480
0.8% La–ZnO	21.24	0.3250	0.5138	0.0477
1.0% La–ZnO	20.58	0.3267	0.5182	0.0472

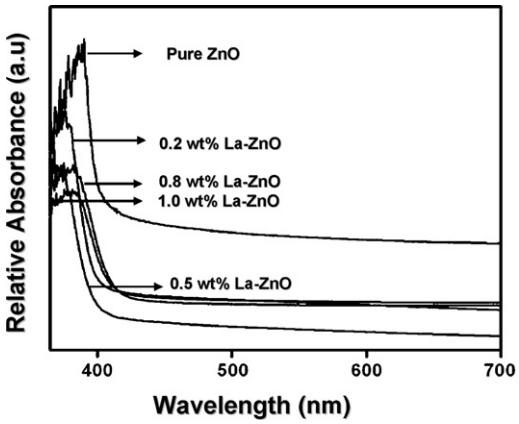

Fig. 3. UV–vis absorption spectra of pure ZnO and La-doped ZnO catalysts.

band shifts toward lower wavelength by about 14–22 nm upon increasing the La loading. Consequently, the band gap of La-doped ZnO also increases gradually with increasing the La loading and is much higher as compared to that of pure ZnO. This could be mainly attributed to the quantum size effect as well as the strong interaction between the surface oxides of Zn and La. These observations strongly suggest that the La doping significantly affects the particle size and hence the absorbance properties. Moreover, these results are in good agreement with the conclusion derived from the XRD results and a similar result has also been reported in La-doped TiO_2 by Liqiang et al. [24].

3.1.3. Atomic force microscope (AFM) analysis

The atomic force microscopic (AFM) images of ZnO and 0.8 wt% La-doped ZnO are presented in Figs.4a and 5a, respectively. The surface roughness profile of ZnO and La-doped ZnO is shown in Figs. 4b and 5b, respectively. Smooth surface is clearly evident for ZnO whereas La-doped ZnO appears rough and porous. The roughness value derived from surface roughness profile is 0.591 nm for ZnO whereas the roughness value for La-doped ZnO is 21.64 nm. The high surface roughness and small particle size of La-doped ZnO reveals higher porosity and surface area than ZnO. It has been reported that the surface area and porosity of the catalysts are important parameters to enhance the activity of the photocatalysts [32]. Thus, we believe that the high surface roughness of La-doped ZnO may be helpful to enhance its photocatalytic activity.

Table 2
UV–vis absorption data for pure ZnO and La-doped ZnO catalysts

Catalyst	λ_{max} (nm)	Bandgap (eV)	Apparent rate constant, *k* ($\times 10^{-2}$ min^{-1})
Pure ZnO	390	3.18	5.25
0.2% La–ZnO	376	3.30	5.42
0.5% La–ZnO	376	3.30	6.61
0.8% La–ZnO	374	3.32	10.09
1.0% La–ZnO	368	3.37	8.01

3.1.4. X-ray photoelectron spectroscopy (XPS) analysis

The nature and the coordination of the elements present in the ZnO and La-doped ZnO were analyzed by X-ray photoelectron spectroscopy (XPS). Fig. 6A shows the Zn LMM spectra of ZnO compared to La-doped ZnO. The spectrum of ZnO exhibits two components with the binding energy values of 265 and 262 eV. The Zn LMM peak at 265 eV is assigned to Zn–O–Zn while the broad peak at 262 eV is attributed to the dissociative Zn atoms or Zn interstitials [33–35]. It is interesting to note that the Zn LMM spectrum of La-doped ZnO is much broader as compared to that of pure ZnO. This could be mainly attributed to the existence of Zn–O–La bonding and difference in the electronegativity of

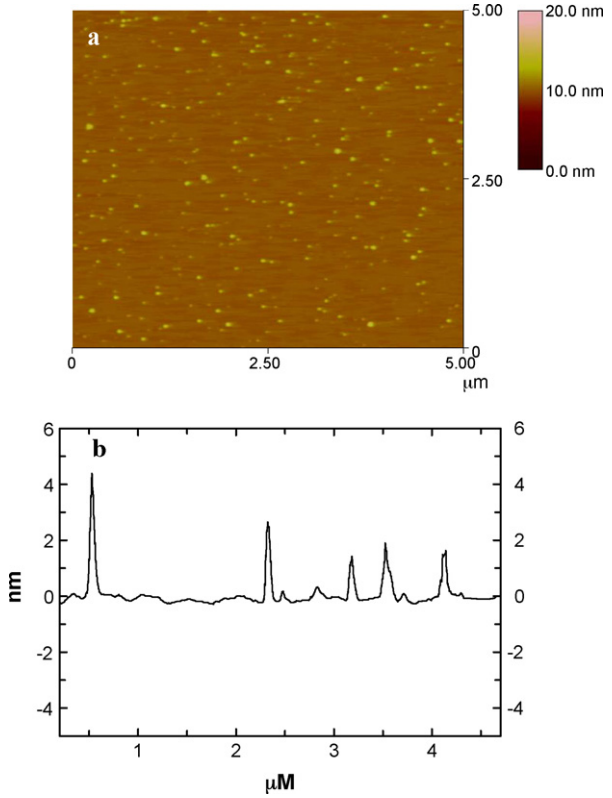

Fig. 4. (a) AFM images of pure ZnO and (b) surface roughness profile of pure ZnO.

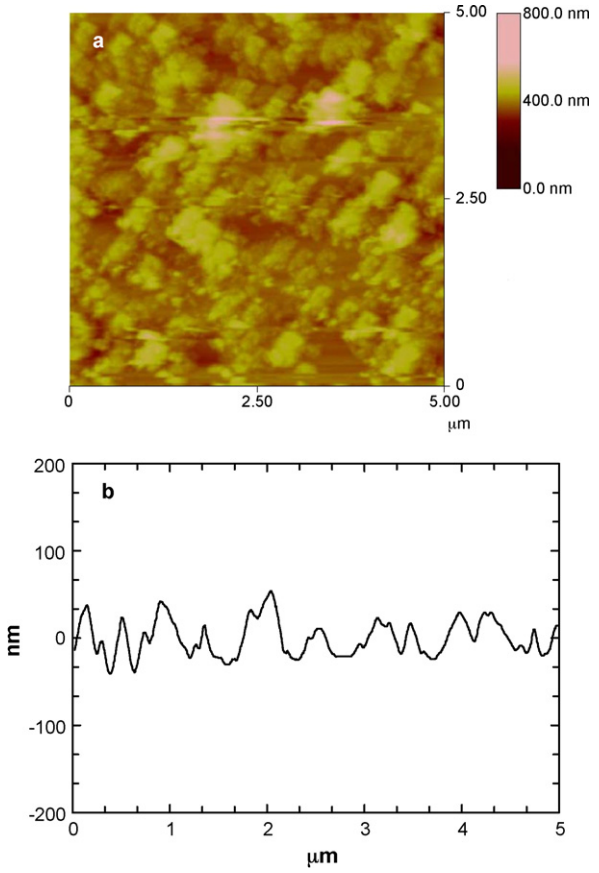

Fig. 5. (a) AFM images of 0.8 wt% La-doped ZnO and (b) surface roughness profile of 0.8 wt% La-doped ZnO.

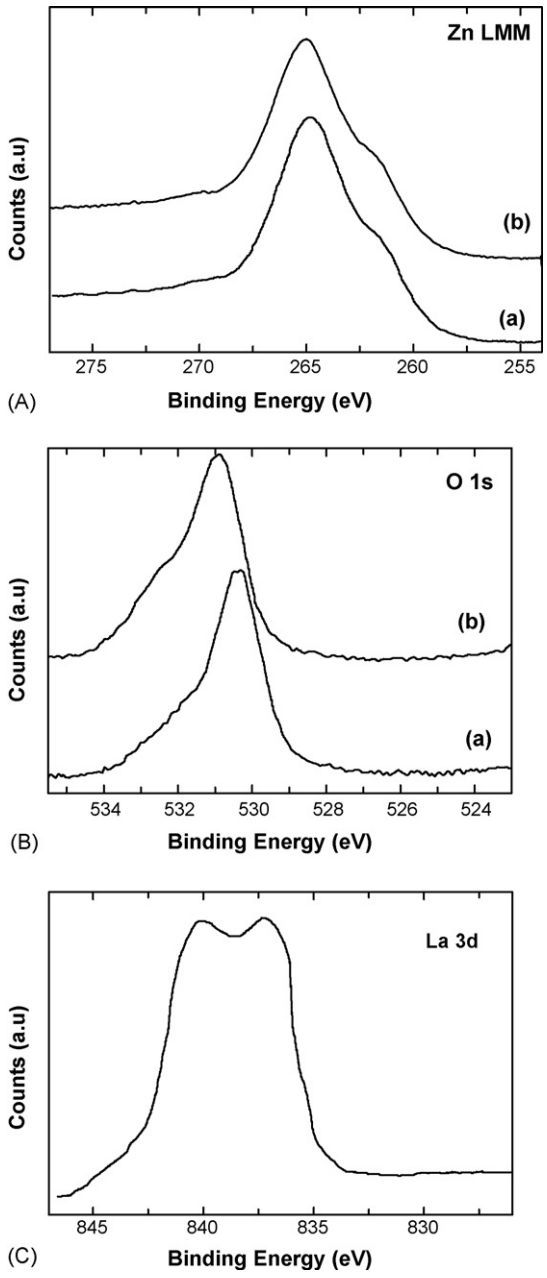

Fig. 6. XPS spectra of pure and 0.8 wt% La-doped ZnO: (A) Zn LMM (*a* = ZnO; *b* = 0.8 wt% La–ZnO); (B) O 1s (*a* = ZnO; *b* = 0.8 wt% La–ZnO) and (C) La 3d.

La and Zn. The O 1s core level spectrum of ZnO and La-doped ZnO is shown in Fig. 6B. The O 1s spectrum of ZnO shows a sharp peak centered around 530.4 eV, which is mainly assigned to the oxygen atoms coordinated with Zn atoms. In the case of La-doped ZnO, a slight shift in the value of the binding energy of the sharp peak (530.8 eV) as well as an additional shoulder centered around 532.5 eV was observed. The peaks which are centered around 530.8 and 532. 5 eV may be attributed to the coordination of oxygen in La–O–La and La–O–Zn, respectively. The La 3d spectrum of La-doped ZnO is shown in Fig. 6C. The spectrum exhibits two components with the binding energy values of 837.3 and 840.2 eV. The highest energy contribution is assigned to the bonding between lanthanum and zinc while the lowest energy contribution is attributed to the bonding in the lanthanum oxide clusters. These results demonstrated that the bonding between the lanthanum and zinc is occurred and the interaction between the lanthanum oxide clusters and the ZnO surface are strongly developed.

3.1.5. HR-SEM analysis of ZnO and La-doped ZnO

The high resolution scanning electron micrograph (HR-SEM) image of ZnO and 0.8 wt% La-doped ZnO is shown in Fig. 7a and b, respectively. HR-SEM image of ZnO nanoparticles illustrates that the morphology is well ordered and the size of the particles are in the range 100–500 nm, suggesting a wide range of band gap value in the ZnO crystals. The HR-SEM image of La-doped ZnO demonstrates that lanthanum oxide clusters are formed on the clear smooth surface of ZnO and show aggregations.

3.2. Adsorption of MCP over ZnO and La-doped ZnO

Adsorption is one of the important aspects in photocatalysis. Hence, prior to photocatalytic experiments, adsorption (dark) experiments were carried out with 100 ml MCP solution over ZnO or La-doped ZnO catalysts. The resulting solution was stirred on a magnetic stirrer and the aliquots were withdrawn at regular intervals for analysis. The percentage of the adsorption of MCP over La-doped ZnO is around 8% whereas only 1.5%

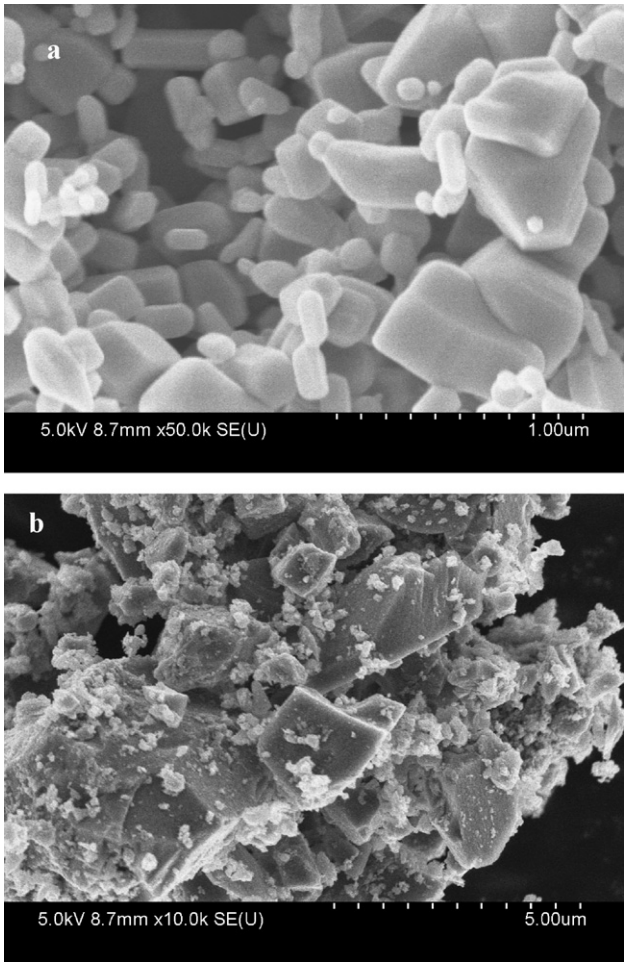

Fig. 7. HR-SEM pictures of (a) pure ZnO and (b) 0.8 wt% La-doped ZnO.

is observed for pure ZnO. The adsorption capacity of La-doped ZnO is much higher as compared to that of pure ZnO.

3.3. Photocatalytic degradation of MCP

In order to determine the photocatalytic activity of ZnO and La-doped ZnO, a series of experiments were carried out with MCP in aqueous suspension with the light of wavelengths 254 and 365 nm. The photocatalytic degradation follows a pseudo-first order reaction and its kinetics can be expressed using $\ln(C_0/C_t) = kt$, where k is the apparent reaction rate constant, C_0 the initial concentration of MCP, t the reaction time and C_t is the concentration of MCP at the reaction time t. Fig. 8 shows the kinetic fit for the degradation of MCP over pure ZnO and La-doped ZnO with different lanthanum loading. The integral linear transform $\ln(C_0/C)$ as a function of time $f(t_R)$ reveals the apparent first order reaction kinetics. The apparent reaction rate constants (k) and $t_{1/2}$ values of ZnO, TiO_2 and La-doped ZnO are presented in Table 3. It is clearly seen from Fig. 8 and Table 3 that the rate of photocatalytic degradation of La-doped ZnO catalysts is much higher as compared to that of pure ZnO and TiO_2. It is interesting to note that the rate constant of the catalysts increases with increasing the La loading up to 0.8 wt% and then decreases. Among the catalysts studied, 0.8 wt% La-doped ZnO

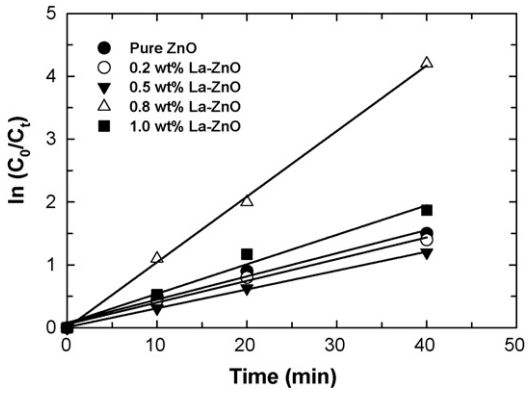

Fig. 8. Kinetic fit for the degradation of MCP with pure ZnO and La-doped ZnO catalysts (initial concentration of MCP = 40 mg l^{-1}; pH 5.3; catalyst amount = 0.1 g/100 ml).

is found be more active, showing high photocatalytic activity for the degradation of MCP. Thus, it is concluded that the optimum loading of La is 0.8 wt% which may be more efficient for separating photoinduced electron–hole pairs and enhance the photocatalytic activity. The reason for the high activity of 0.8 wt% La-doped ZnO and the effect of La loading on the photocatalytic activity can be explained as follows: Pleskov [36] reported that the value of space charge region potential for efficient separation of electron–hole pairs should not be lower than 0.2 V. The increase in La^{3+} ion concentration the surface barrier becomes higher, the space charge region becomes narrower and hence the electron–hole pairs are efficiently separated by the large electric field. On the other hand, with increase in concentration of La^{3+} ions, the penetration depth of light into ZnO can greatly exceed the space charge layer. Therefore, the recombination of photogenerated electron–hole pairs becomes easier. It should be noted that the band-bending and the electrical field of the ZnO colloidal particles are very small while the band gap energies of rare earth oxides in general and La_2O_3 in particular are not sufficient for photocatalytic reactions. However, an optimum concentration of La^{3+} ions is required to match the thickness of charge layer and the depth of the light penetration for separating photo-induces electron–hole pairs. In addition, appropriate loading of La^{3+} ions is highly necessary for producing a significant potential difference between the surface and the center of the particles in order to efficiently separate the pho-

Table 3
Apparent kinetic values for the degradation of MCP

Catalysts	Apparent kinetic constant, k ($\times 10^{-2}$ min^{-1})	$t_{1/2}$ values (min)	Correlation co-efficient (R^2 value)
Pure ZnO	5.25	13.20	0.976
0.2% La–ZnO	5.42	12.79	0.987
0.5% La–ZnO	6.61	10.48	0.999
0.8% La–ZnO	10.09	6.87	0.959
1.0% La–ZnO	8.01	8.65	0.977
Pure TiO_2	6.0	11.55	0.985

MCP = 40 mg l^{-1}; ZnO, TiO_2 or La–ZnO = 100 mg/100 ml; pH 5; UV = 8 lamps; λ = 254 nm; adsorption equilibrium = 30 min; irradiation = 60 min.

Table 4
Apparent kinetic values for the degradation of monocrotophos

Catalysts	Apparent kinetic constant, k ($\times 10^{-2}$ min^{-1})	$t_{1/2}$ values (min)	Correlation co-efficient (R^2 value)
Pure ZnO	3.00	13.20	0.999
0.2% La–ZnO	5.42	12.79	0.995
0.5% La–ZnO	6.61	10.48	0.993
0.8% La–ZnO	8.27	8.38	0.994
1.0% La–ZnO	8.00	8.66	0.985
Pure TiO_2	5.3	13.08	0.999

MCP = 40 mg l^{-1}; ZnO, TiO_2 or La–ZnO = 100 mg/100 ml; pH 5; UV = 8 lamps; λ = 365 nm; adsorption equilibrium = 30 min; irradiation = 60 min.

toinduced electron–hole pairs [37] because the excess La_2O_3 covering the surface of ZnO may increase the number of recombination centers, thus, giving low photocatalytic activity. This can be clearly seen from the present study that La-doped ZnO with more than 0.8 wt% of La loading showed a very low photocatalytic activity. The higher activity of 0.8 wt% La-doped ZnO can be attributed to a strong absorption of OH^- ions on the surface of ZnO because of a large number of oxygen vacancies. These OH^- ions are assumed to serve as surface bound traps for the photogenerated holes, which prevent electron–hole recombination. A similar behavior has also been reported in La-doped TiO_2.

The photocatalytic activity with the light of wavelength 365 nm (Table 4) is less than that of wavelength 254 nm. This difference is due to enhanced electron–hole recombination with light of wavelength 365 nm. But the light of wavelength 254 nm can excite electrons with high kinetic energy and hence they can easily escape electron–hole recombination. The optimum La-loading for both 254 and 365 nm was found to be 0.8 wt%. The $t_{1/2}$ values of 0.8 wt% La-doped ZnO are 8.38 and 6.9 for 254 and 365 nm, respectively, suggesting that La-doped ZnO exhibits higher photocatalytic activity as compared to pure ZnO and TiO_2. The plot of experimentally and theoretically derived values of C/C_0 versus time for ZnO and La-doped ZnO catalysts are depicted in Fig. 9. The experimentally derived points are exactly coinciding with the theoretical curve illustrating that the reaction follows first-order kinetics.

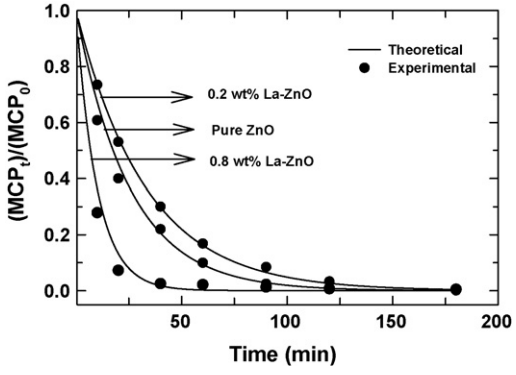

Fig. 9. Effect of irradiation time in the degradation of MCP (initial concentration of monocrotophos 40 mg l^{-1}; pH 5.3; catalyst amount = 0.1 g/100 ml).

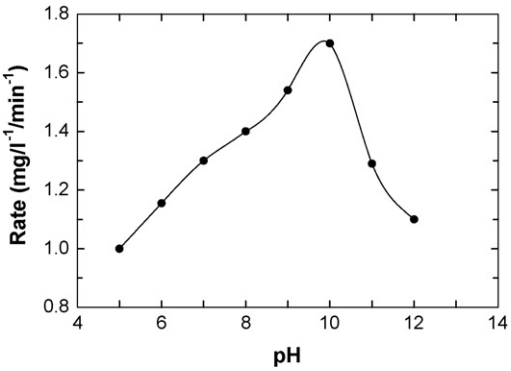

Fig. 10. Effect of solution pH on the rate of degradation (concentration of MCP = 40 mg l^{-1}; catalyst amount = 0.1 g/100 ml).

3.4. Effect of pH

The solution pH exhibits profound influence on ZnO oxidation potential and surface charge, which affect adsorption and degradation of MCP. Hence, the role of pH on the degradation rate was studied in the pH range 5–12 with 40 mg l^{-1} initial concentration of MCP and 0.1 g/100 ml catalyst. The influence of solution pH on the degradation rate of MCP is depicted in Fig. 10. It shows that the rate of degradation increases gradually with increasing the solution pH up to 8 and increases rapidly above the solution pH of 8, and reaches a maximum value approximately at pH 10. The photocatalytic degradation of MCP is strongly favored in alkaline pH. Sakthivel et al. [5] have observed similar trend with ZnO and further demonstrated that acid-base property of the metal oxide surfaces influence considerable implication upon their photocatalytic activity. The high degradation rate at pH 10 is explained as follows. The zero point charge of ZnO is 9.0 ± 0.3 and above this value, the surface is negatively charged due to adsorbed OH^- ions. The presence of large quantities of adsorbed OH^- ions on the particle surface favors the formation of $^{\bullet}OH$ radicals, which is accepted as the primary oxidizing species responsible for degradation [7,38]. On the other hand, a noticeable decrease in the rate of degradation above pH 10 is observed as shown in Fig. 10. This is due to decrease in the adsorption of MCP. Above pH 10, the catalyst surface may adsorb OH^- ions and thus it becomes negatively charged. Since MCP is not protonated above pH 10, the electrostatic repulsion between the surface charges on the adsorbent and the adsorbate hinders the amount of MCP adsorption. Consequently, the degradation rate decreases above pH 10. The decrease in the photocatalytic degradation in the acidic medium is due to a high adsorption of MCP [39]. As the catalyst surface is fully covered by MCP, absorption of UV radiation on the catalyst surface decreases, which is very important for the photocatalytic process.

3.5. Photocatalytic mineralization of MCP in aqueous suspension

Complete mineralization of pollutants with cost-effective process is important for industrial applications. The HPLC chromatograms revealed that MCP molecules are degraded in to

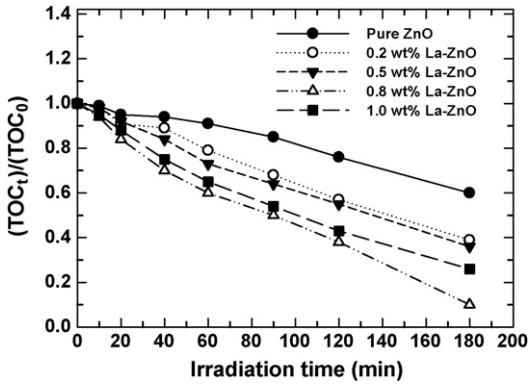

Fig. 11. Comparison of photocatalytic mineralization of pure ZnO and La-doped ZnO (MCP concentration = 40 mg l^{-1}; catalyst amount = 100 mg/100 ml; solution pH 10; λ = 254 nm).

smaller fragments and subsequently mineralized completely (not shown). The TOC concentration of MCP decreases significantly with increasing the irradiation time for the light of wavelengths 254 and 365 nm as shown in Figs. 11 and 12, respectively. As irradiation time increases, MCP degrades into small fragments and consequently complete mineralization is achieved in about 120 min. La-doped ZnO photocatalysts require shorter irradiation time for complete mineralization than pure ZnO. This is due to suppression of electron–hole recombination and generation of more •OH radicals. The •OH radicals are strong enough to break different (C–C, C=C, and C=O) bonds in MCP molecules adsorbed on the surface of ZnO, and this will lead to the formation of CO_2 and inorganic ions at the end. Further, continuous degradation of MCP leads to the formation of intermediates such as aldehydes, alcohols, nitrates and phosphoric acid. The alcohol and aldehydes can easily be hydrolyzed in water whereas the phosphoric acid and nitrates are transformed into harmless inorganic ions such as phosphates (PO_4^{3-}) and nitrates (NO_3^-). Finally, MCP and its intermediate are converted into CO_2, H_2O and harmless inorganic ions.

The rate of mineralization was high in the initial period followed by the slow rate. This slow rate indicates the formation of a few long-lived by-products, which had a low rate of reaction with hydroxyl radicals. This reveals the formation of intermediates and their competitiveness with MCP anions in the photocatalytic

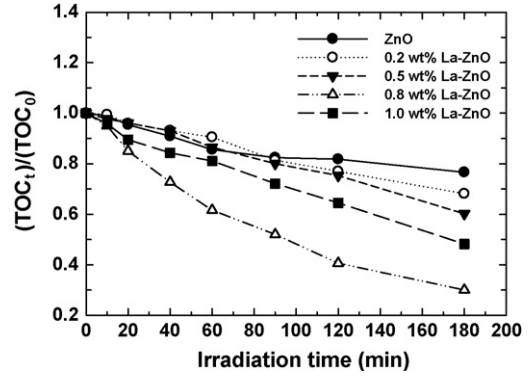

Fig. 12. Comparison of photocatalytic mineralization of pure ZnO and La-doped ZnO catalysts (MCP concentration = 40 mg l^{-1}; catalyst amount = 100 mg/100 ml; solution pH 10; λ = 365 nm).

Table 5
Comparison of relative photonic efficiencies in the photodegradation of MCP by ZnO and La-doped ZnO photocatalysts

Catalysts	Relative photonic efficiency (ξ_r)	
	254 nm	365 nm
Pure ZnO	1.03 ± 0.01	0.76 ± 0.01
0.2% La–ZnO	1.10 ± 0.01	0.89 ± 0.01
0.5% La–ZnO	1.26 ± 0.01	0.91 ± 0.01
0.8% La–ZnO	2.54 ± 0.01	1.57 ± 0.01
1.0% La–ZnO	1.51 ± 0.01	1.25 ± 0.01
Commercial ZnO	1.00 ± 0.01	1.00 ± 0.01
TiO_2	1.36 ± 0.01	1.01 ± 0.01

MCP = 40 mg l^{-1}; ZnO, TiO_2 or La–ZnO = 100 mg/100 ml; pH 5; UV = 8 lamps; λ = 254 and 365 nm; adsorption equilibrium = 30 min; irradiation = 60 min.

degradation. Release of PO_4^{3-} ions during degradation of MCP reduces the reaction rate as PO_4^{3-} gets adsorbed on catalyst surface. Abdullah et al. [40] reported that sulfate and phosphate ions inhibited the photocatalytic oxidation of organic solutes and reduced the rate up to 70%. Such type of hindering effects has been already reported in the photocatalytic degradation of textile dyes [41]. This decrease in the reaction rate can also be attributed to low reactivity of short chain aliphatic compounds with •OH radicals [42]. The TOC removal for the light of wavelength 254 nm (Fig. 11) after 120 min with pure ZnO, 0.2, 0.5, 0.8, and 1.0 wt% La-doped ZnO catalysts is found to be 24, 61, 78, 100, and 74%, respectively. Similarly the TOC removal for the light of wavelength 365 nm (Fig. 12) with pure ZnO, 0.2, 0.5, 0.8, and 1.0% La-doped ZnO catalysts is found to be 15, 41, 60, 80, and 55%, respectively. These results demonstrated that the photocatalytic activity of 0.8 wt% La-doped ZnO is much higher as compared to that of other catalysts.

3.6. Relative photonic efficiency

In order to evaluate the relative photonic efficiency (ξ_r), a solution of MCP (40 mg l^{-1}) adjusted to pH 10 was irradiated with 100 mg ZnO (Merck) or La-doped ZnO. The relative photonic efficiencies of light of wavelengths 254 and 365 nm for ZnO and La-doped ZnO are presented in Table 5. For comparison, the relative photonic efficiency of TiO_2 is also presented in Table. The relative photonic efficiencies of La-doped ZnO are greater as compared to those of ZnO and TiO_2, revealing the effectiveness of metal-doped systems. It is also interesting to note that the relative photonic efficiency for La-doped ZnO for light of wavelength 254 nm are much higher as compared to that for 365 nm. The results are in good agreement with degradation and mineralization studies. Comparing the high efficiency of La-doped ZnO catalysts with standard ZnO and TiO_2 catalyst, the photocatalytic efficiency of 0.8 wt% La-doped ZnO is about 2.5 and 1.5 times higher as compared to that of ZnO and TiO_2 with light of wavelengths 254 and 365 nm, respectively.

4. Conclusion

A series of La-doped ZnO with different La loading were prepared and unambiguously characterized by XRD, UV–vis,

AFM, XPS, and HR-SEM. It was found that La^{3+} is uniformly dispersed on ZnO nanoparticles in the form of small La_2O_3 cluster. The XRD and UV–vis results revealed that the particle size of La-doped ZnO is much smaller as compared to that of pure ZnO and decreases with increasing La loading. Rough and high porous surface of La-doped ZnO was observed by AFM, which is critical for enhancing the photocatalytic activity. The photocatalytic activity of La-doped ZnO for the degradation of MCP was studied and the results are compared with ZnO and TiO_2. It was observed that the rate of degradation of MCP over La-doped ZnO increases with increasing La loading up to 0.8 wt% and then decreases. The TOC results demonstrated that La-doped ZnO requires shorter irradiation time for the complete mineralization of MCP than pure ZnO. The relative photonic efficiencies and the photocatalytic activity of the 0.8 wt% La-doped ZnO are much higher as compared to those of pure ZnO and TiO_2. It was concluded that small particle size, separation of charge carriers (e^-/h^+), rough and high porous surface of La-doped ZnO are the major constituents for its enhanced photocatalytic activity in the present study.

Acknowledgements

The authors acknowledge the University Grants Commission, New Delhi for the liberal funding through Centre with Potential for Excellence in Environmental Science (CPEES) at our University. The authors express their gratitude for the support and encouragement of the CPEES Director, Prof. G.M. Samuel Knight. One of the authors (S. Anandan) is grateful to UGC, New Delhi and CPEES, Anna University, Chennai for providing stipend to carryout the research work.

References

[1] M.R. Hoffmann, S.T. Martin, W.Y. Choi, D.W. Bahnemann, Chem. Rev. 95 (1995) 69.
[2] T. Sehili, P. Boule, J. Lemaire, J. Photochem. Photobiol. A: Chem. 50 (1989) 103.
[3] J. Villasenor, P. Reyes, G. Pecchi, J. Chem. Technol. Biotechnol. 72 (1998) 105.
[4] M.D. Driessen, T.M. Miller, V.H. Grassian, J. Mol. Catal. A: Chem. 131 (1998) 149.
[5] S. Sakthivel, B. Neppolian, M.V. Shankar, B. Arabindoo, M. Palanichamy, V. Murugesan, Sol. Energy Mater. Sol. Cells 77 (2003) 65.
[6] M.L. Curri, R. Comparelli, P.D. Cozolli, G. Mascolo, A. Agostiano, Mater. Sci. Eng. C 23 (2003) 285.
[7] A.A. Khodja, T. Sehili, J.F. Pilichowski, P. Boule, J. Photochem. Photobiol., Part A: Chem. 141 (2001) 231.
[8] I. Poulios, I. Tsachpinis, J. Chem. Technol. Biotechnol. 74 (1999) 349.
[9] A. Sharma, P. Rao, R.P. Mathur, S.C. Ameta, J. Photochem. Photobiol. A: Chem. 86 (1995) 197.
[10] P.V. Kamath, R. Huehn, R. Nicolaesscu, J. Phys. Chem. B 106 (2002) 788.
[11] E.G. Bylander, J. Appl. Phys. 49 (1978) 1188.
[12] B. Lin, Z. Fu, Y. Zia, Appl. Phys. Lett. 79 (2001) 943.
[13] A.L. Linsebigler, G.Q. Lu, J.T. Yates Jr., Chem. Rev. 95 (1995) 735.
[14] M. Romero, J. Blanco, B. Sanchez, A. Vidal, S. Malato, A.I. Cardona, E. Garcia, Solar Energy 66 (1999) 169.
[15] J. Moser, S. Punchihewa, P.P. Infelta, M. Graetzel, Langmuir 7 (1991) 3012.
[16] A.P. Hong, D.W. Bahnemann, M.R. Hoffmann, J. Phys. Chem. 91 (1987) 2109.
[17] J. Lin, J.C. Yu, D. Lo, S.K. Lam, J. Catal. 183 (1999) 368.
[18] N. Serpone, D. Lawless, J. Disdier, J.M. Hermann, Langmuir 10 (1994) 643.
[19] J. Lin, J.C. Yu, J. Photochem. Photobiol. A: Chem. 116 (1998) 63.
[20] D. Li, H. Haneda, J. Photochem. Photobiol. A: Chem. 155 (2003) 171.
[21] S. Rengaraj, X.Z. Li, Int. J. Environ. Pollut. 27 (2006) 1.
[22] A. Mills, R.H. Davies, D. Worsley, Chem. Soc. Rev. 22 (1993) 417.
[23] A.W. Xu, Y. Gao, H.Q. Liu, J. Catal. 207 (2002) 151.
[24] J. Liqiang, S. Xiaojun, X. Baifu, W. Baiqi, C. Weimin, F. Honggang, J. Solid State Chem. 177 (2004) 3375.
[25] K.T. Ranjit, I. Willner, S.H. Bossmann, A.M. Braun, Environ. Sci. Technol. 35 (2001) 1544.
[26] W.F. Yao, H. Wang, X.H. Xu, X.N. Yang, Y. Zhang, S.X. Shang, M. Wang, Appl. Catal. A: Gen. 251 (2003) 235.
[27] M.V. Shankar, K.K. Cheralthan, B. Arabindoo, M. Palanichamy, V. Murugesan, J. Mol. Catal. 223 (2004) 195.
[28] M.V. Shankar, S. Anandan, N. Venkatachalam, B. Arabindoo, V. Murugesan, Chemosphere 63 (2006) 1014.
[29] T. Nakashima, Y. Ohko, D.A. Tryk, A. Fujishima, J. Photochem. Photobiol. A: Chem. 151 (2002) 207–212.
[30] L.H. Keith, Environmental Endocrine Disrupters—A Handbook of Property Data, John Wiley & Sons, Inc., New York, 1997.
[31] J. Wang, L. Gao, J. Am. Ceram. Soc. 88 (2005) 1637.
[32] M.O. Abou-Helal, W.T. Seeber, Appl. Surf. Sci. 195 (2002) 53.
[33] M. Chen, X. Wang, Y.H. Yu, Z.L. Pei, X.D. Bai, C. Sun, R.F. Huang, L.S. Wen, Appl. Surf. Sci. 158 (2000) 134.
[34] B.M. Ataev, A.D. Bagamadova, V.V. Mamedov, Thin Solid Films 283 (1996) 5.
[35] B. Zhao, H. Yang, G. Du, X. Fang, D. Liu, C. Gao, X. Liu, B. Xie, Semicond. Sci. Technol. 19 (2004) 770.
[36] Y.V. Pleskov, Sov. Eletrochem. 17 (1981) 1.
[37] A. Hagfeldt, M. Graetzel, Chem. Rev. 95 (1995) 49.
[38] M. Muruganandham, M. Swaminathan, Sol. Energy Mater. Sol. Cells 81 (2004) 439.
[39] S. Chakrabarti, B.K. Dutta, J. Hazard. Mater. 112 (2004) 269.
[40] M. Abdullah, G.K.C. Low, R.W. Matthews, J. Phys. Chem. 94 (1990) 6820.
[41] M.V. Shankar, B. Neppolian, B. Arabindoo, M. Palanichamy, V. Murugesan, Indian J. Eng. Mater. Sci. 8 (2001) 104.
[42] C.A. Martin, M.A. Baltanas, A.E. Cassano, J. Photochem. Photobiol., Part A: Chem. 76 (1993) 199.